A New Recovery Strategy of HVDC System during AC Faults

Juanjuan Wang*, Menghua Huang*, Chuang Fu*, *Member*, *IEEE*, Huan Li, Shukai XU, *Senior Member*, *IEEE* and Xiaohua Li

Abstract—**To overcome the disadvantage of VDCOL of HVDC control system, which cannot achieve decoupling control of reactive power and active power, a novel AC fault recovery strategy is proposed in this study. By virtue of such recovery strategy, the exchange of reactive power between the AC system and the converter station can be controlled quantitatively to find the correspondence between DC current order and AC bus voltage. In order to determine the expected reactive power consumption of converters, the instantaneous reactive power theory is used to calculate the reactive power compensated by AC filters. According to the quasi steady-state calculation equations of HVDC system and the operational range of converter firing angle, the constraint relation between the maximum permissible operating value of DC current and AC bus voltage under different AC fault types is obtained. Then by comparing the DC current order and the maximum value of DC current, the smaller of them is taken as the final DC current order so as to improve the recovery performance of the AC-DC system in real time. Finally, the effectiveness and robustness of the proposed control strategy in suppressing subsequent commutation failures and improving the system recovery performance are verified in the CIGRE benchmark model for HVDC controls.**

Index Terms—**HVDC; fault recovery; DC current limit; instantaneous reactive power theory; reactive power control**

I. INTRODUCTION

As high-voltage direct-current system （HVDC） is capable of transmitting bulk power over long distance with low loss, it is being widely employed in the interconnection of power grids [1-4]. However, in case of commutation failure on the inverter side, the safe and stable operation of complicated AC-DC power grids will be greatly affected. This is especially true for the AC-DC system with a weak AC system connected to inverter station or multi-infeed HVDC systems. The main consequences include: 1) If the AC system fault at receiving end is not cleared in time, it may result in subsequent commutation failures, reduction of DC transmission power, DC bias of converter transformer, and voltage instability of weak AC systems on the inverter side [5]; 2) Reactive power balance of the converter station may be upset after AC faults, resulting in excess reactive power or insufficient reactive power which is unfavorable for system recovery and may lead to subsequent commutation failures [6].

The voltage dependent current order limiter (VDCOL) widely used in HVDC transmission projects can improve the fault recovery performance of AC-DC power grids through limiting DC current order under low voltage condition, and many studies on the subject have been conducted. Most relevant studies on VDCOL optimization, however, are performed based on simulation test, which are undesirable in that the parameter values are taken without theoretical basis. In [7], the effect of VDCOL on the recovery performance of AC-DC system is analyzed. In [8], the optimization of the delay time constants of VDCOL in multi-infeed HVDCs is discussed. In [9], an improved current order limiter control for commutation failure mitigation is proposed. In [10], the impact of prediction control and prediction parameters of commutation failure on nonlinear trajectory of reactive power and voltage stability of inverter station is analyzed. In [11], a transient voltage stability control strategy in which the inverter station is taken as dynamic reactive power resource is proposed through simulation tests. In reference [12-13], the impact of the change of extinction angle on reactive power consumption is analyzed through investigating the relationship among reactive power consumption, extinction angle, overlap angle and DC current. In [14], an optimal control strategy is proposed, in which the set value of the extinction angle is adjusted dynamically taking into account the shifting of zero-crossing of commutation voltage on the inverter side and the effect of such optimal control strategy on the operating parameters of HVDC system is analyzed. This control strategy can reduce the probability of HVDC commutation failure to a certain extent. In [15], an optimal strategy for improving the knee point parameters of VDCOL is proposed with the goal of maintaining the reactive power balance of the converter station. In [16], a reactive power

This paragraph of the first footnote will contain the date on which you submitted your paper for review.

This work was supported by National Natural Science Foundation of China(51777079), The State Grid joint funds for smart grid of China （U1766213） and Science and technology project of the Southern Power Grid of China (ZBKJXM20180104).

Juanjuan Wang, Menghua Huang and Xiaohua Li are with the School of Electric Power, South China University of Technology, Guangzhou 510640, China (e-mail: epjjwang@scut.edu.cn; 15367985136@163.com; eplxh@scut.edu.cn).

Chuang Fu, Huan Li and Shukai XU is with the State Key Laboratory of HVDC, Electric Power Research Institute, China Southern Power Grid, Guangzhou 510663, China(e-mail: fuchuang@csg.cn, lihuan3@csg.cn, xusk@csg.cn).

*These three authors equally contributed to this work.

This article has been accepted for publication in a future issue of this journal, but has not been fully edited. Content may change prior to final publication. Citation information: DOI 10.1109/TPWRD.2019.2892410, IEEE Transactions on Power Delivery

control strategy is proposed, in which the reactive power regulation capability of converters is utilized. In [17], a design method of VDCOL parameters is proposed with an objective function considering minimum sum of reactive power demand peaks of MIDC recovery.

Although the above studies have improved the recovery performance of AC-DC systems after AC faults from various aspects, they fail to break the constraints imposed on the VDCOL control. Specially, without regard to the variation characteristics and the interactions among electrical quantities after AC faults, these studies fail to decouple the active and reactive power of converter station and make full use of the reactive power control capability of converters. It is therefore necessary to conduct systematic and in-depth studies on operating characteristics of HVDC transmission system to develop a convictive and widely applicable AC fault recovery strategy.

In this paper, the characteristic relationship among AC bus voltage, the reactive power of converter station and DC current in case of AC fault is quantitatively analyzed, the operation mechanism and drawbacks of VDCOL are explored and a control strategy which is effective in suppressing continuous commutation failures of HVDC system is proposed. The DC current order is constrained by considering the variation characteristics of electrical angles and their interactions after AC faults. Finally, the proposed control strategy is applied to the CIGRE benchmark model for HVDC controls and the test results have verified the effectiveness of the control strategy in enhancing the recovery performance of AC-DC transmission systems.

The remainder of the paper is organized as follows. In Section II, a new AC fault recovery strategy based on reactive power control at converter stations is proposed. In Section III, the limit values of DC current order under different AC faults are analytically derived. In Section V, the test results of the proposed recovery strategy are presented. The general conclusions are summarized in Section V.

II. AC Fault Recovery Strategy Based on Reactive Power Control at Converter Stations

A. *Reactive Power Characteristics of Converter Station*

In HVDC transmission system, reactive power balance between the converter station and the AC system is shown in Fig.1 [17].

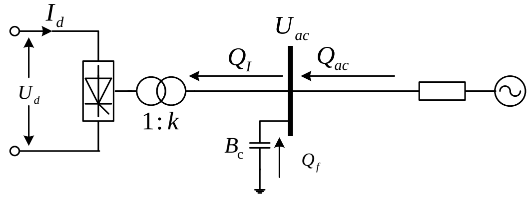

Fig. 1 Reactive power balance of converter station

In Fig.1, U_{ac} is the voltage RMS on AC bus, I_d is DC current, U_d is DC voltage, Q_f is the reactive power supplied by AC filters, Q_I is the reactive power consumed by the inverter, Q_{ac} is the exchange of reactive power between converter station and AC system. As shown in Fig. 1, the formula of reactive power balance of converter stations is:

$$Q_{ac} + Q_f = Q_I \tag{1}$$

A negative value of Q_{ac} indicates that the AC system absorbs reactive power from the converter station. Conversely, a positive value of Q_{ac} indicates that the AC system supplies reactive power to the converter station.

Reactive power consumed by the inverter is calculated using Equation (2) [18]:

$$Q_I = \sqrt{\begin{array}{l}[(\frac{3\sqrt{2}}{\pi}k)^2 - (\frac{3\sqrt{2}}{\pi}k\cos\gamma)^2]N_p^2U_{ac}^2I_d^2 + \\ \frac{18\sqrt{2}kX\cos\gamma}{\pi^2}N_p^2U_{ac}I_d^3 - (\frac{3N_pXI_d^2}{\pi})^2\end{array}} \tag{2}$$

where, γ is the extinction angle on the inverter side, k is the turns ratio of converter transformer, N_p is the number of pole pairs, X is the equivalent short-circuit impedance on the secondary side of the transformer. If AC faults occur on the inverter side, the rectifier will operate under constant-current control mode and the inverter will operate under constant-extinction-angle control mode. When the system enters the quasi-steady state, the reactive power supplied by the AC filters can be calculated using:

$$Q_f = B_cU_{ac}^2 \tag{3}$$

where, B_c is the equivalent susceptance of the AC filters. Taking the CIGRE model for example, k, N_p, X, γ, and B_c in Equations (2) and (3) are all constants. By substituting Equations (2) and (3) into Equation (1), one can obtain the distribution profile of reactive power exchange Q_{ac} with different U_{ac} and I_d, as shown in Fig.2(a).

In the CIGRE HVDC model, the U_d-I_d characteristic function of VDCOL is given by:

$$I_d = \begin{cases} 1.1(U_d \le 200kV) \\ 0.0036U_d + 0.380(200kV < U_d < 450kV) \quad (kA) \\ 2(U_d \ge 450kV) \end{cases} \tag{4}$$

where,

$$U_d = 2(\frac{3\sqrt{2}}{\pi}kU_{ac}\cos\gamma - \frac{3}{\pi}XI_d) \tag{5}$$

By substituting Equation (5) as well as the parameters of CIGRE HVDC model into Equation (4), the I_d-U_{ac} characteristic function of VDCOL can be obtained, and its per-unit value expression is given by:

$$I_d = \begin{cases} 0.55(U_{ac} \le 0.4p.u.) \\ 0.92U_{ac} + 0.177(0.4 < U_{ac} < 0.9p.u.) \\ 1(U_{ac} \ge 0.9p.u.) \end{cases} \tag{6}$$

Then by substituting Equations (2), (3), (6) and CIGRE model parameters into Equation (1), one can obtain the constraint relationship between Q_{ac} and U_{ac} under the VDCOL control, as shown in Fig.2(b).

This article has been accepted for publication in a future issue of this journal, but has not been fully edited. Content may change prior to final publication. Citation information: DOI 10.1109/TPWRD.2019.2892410, IEEE Transactions on Power Delivery

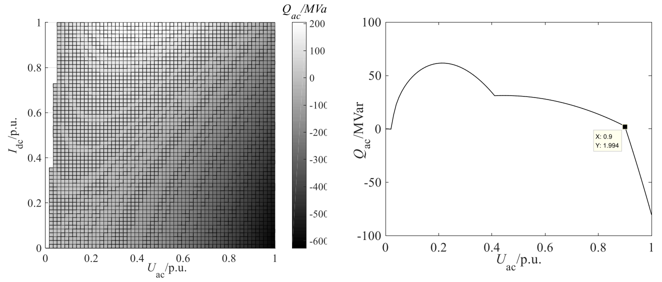

(a) under different U_{ac} and I_d (b) under the VDCOL control

Fig.2 Distribution profile of reactive power exchange

In Fig.2(b), with a small magnitude decline of AC voltage, the exchanged reactive power between the converter station and the AC system is capacitive. Namely, the surplus reactive power supplied by the AC filter flows into the AC system to support the AC voltage stability. In contrast, with a larger magnitude decline of AC voltage, the exchanged reactive power between the converter station and the AC system becomes inductive and gradually increases. Namely, as the fault becomes more severe, the reactive power supplied from the AC filter to the converter station becomes deficient and the transmission of reactive power from the AC system to the converter station is started. If such operating condition sustains for a long time, it will be extremely unfavorable for stable operation of HVDC transmission system.

B. Determination of Reactive Power Compensated by AC Filter

When HVDC transmission systems operate under the quasi-steady state, the reactive power supplied by the AC filters can be dynamically calculated using Equation (3). However, in case of asymmetrical faults in AC system or during the transient process of faults, Q_f calculated by Equation (3) will be no longer accurate. Therefore, the instantaneous value of reactive power supplied by the AC filter is calculated based on the instantaneous reactive power theory [19]. As reactive power is not related to zero sequence component, the AC three-phase voltages (v_a, v_b and v_c) and currents (i_a, i_b and i_c) of AC filters measured in real time can be expressed in terms of the sum of positive and negative sequence components of each harmonics. Taking fundamental component of voltage for example, it can be expressed as:

$$\begin{bmatrix} v_a \\ v_b \\ v_c \end{bmatrix} = \begin{bmatrix} v_a^+ \\ v_b^+ \\ v_c^+ \end{bmatrix} + \begin{bmatrix} v_a^- \\ v_b^- \\ v_c^- \end{bmatrix} \tag{7}$$

Through the Park's transformation, Equation (7) turns into Equation (8):

$$\vec{\boldsymbol{v}} = \begin{bmatrix} v_d \\ v_q \end{bmatrix} = \begin{bmatrix} v_d^+ + v_d^- \\ v_q^+ + v_q^- \end{bmatrix} = \boldsymbol{T}_{park} \begin{bmatrix} v_a^+ + v_a^- \\ v_b^+ + v_b^- \\ v_c^+ + v_c^- \end{bmatrix} \tag{8}$$

where, $\boldsymbol{T}_{park}$ is Park′s transformation matrix:

$$\boldsymbol{T}_{park} = \sqrt{\frac{2}{3}} \begin{bmatrix} \cos\omega t & \cos(\omega t - 120°) & \cos(\omega t + 120°) \\ -\sin\omega t & -\sin(\omega t - 120°) & -\sin(\omega t + 120°) \end{bmatrix}$$

Then, the vector of three-phase voltage $\vec{v}$ can be expressed as:

$$\vec{\boldsymbol{v}} = \vec{\boldsymbol{v}}_{dq}^+ + \vec{\boldsymbol{v}}_{dq}^- = (\vec{\boldsymbol{v}}_d^+ + \vec{\boldsymbol{v}}_q^+) + (\vec{\boldsymbol{v}}_d^- + \vec{\boldsymbol{v}}_q^-) \tag{9}$$

Similarly, the vector of three-phase current $\vec{i}$ can be expressed as:

$$\vec{\boldsymbol{i}} = \vec{\boldsymbol{i}}_{dq}^+ + \vec{\boldsymbol{i}}_{dq}^- = (\vec{\boldsymbol{i}}_d^+ + \vec{\boldsymbol{i}}_q^+) + (\vec{\boldsymbol{i}}_d^- + \vec{\boldsymbol{i}}_q^-) \tag{10}$$

In Equations (9) and (10), $\vec{\boldsymbol{v}}_{dq}^+$ and $\vec{\boldsymbol{v}}_{dq}^-$ are respectively the positive and negative sequence components of AC filter three-phase voltage (namely the AC bus three-phase voltage), and $\vec{\boldsymbol{i}}_{dq}^+$ and $\vec{\boldsymbol{i}}_{dq}^-$ are respectively the positive and negative sequence components of AC filter three-phase current. The positions of the positive and negative sequence components on dq rotational coordinate axis are shown in Fig.3.

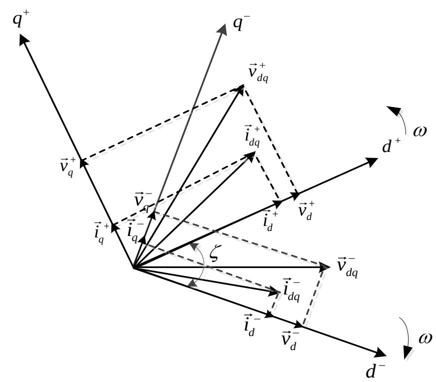

Fig. 3. The sequence components on dq rotational coordinate axis

In Fig.3, positive sequence component rotates counterclockwise at angular velocity ω with the positive dq rotational coordinate axis, while negative sequence component rotates clockwise at angular velocity ω with the negative dq rotational coordinate axis. The angle difference between d^+ coordinate axis and d^- coordinate axis may be expressed as ξ. Based on the vector algorithm, the three-phase instantaneous reactive power q can be obtained as:

$$\begin{aligned} q &= \vec{\boldsymbol{v}} \times \vec{\boldsymbol{i}} \\ &= (\vec{\boldsymbol{v}}_d^+ + \vec{\boldsymbol{v}}_q^+ + \vec{\boldsymbol{v}}_d^- + \vec{\boldsymbol{v}}_q^-) \times (\vec{\boldsymbol{i}}_d^+ + \vec{\boldsymbol{i}}_q^+ + \vec{\boldsymbol{i}}_d^- + \vec{\boldsymbol{i}}_q^-) \end{aligned} \tag{11}$$

In Equation (11), the DC component of q is denoted as $\bar{Q}_0$, the coefficient of the cosine component of q is denoted as $\tilde{Q}_{\cos}$, the coefficient of the sinusoidal component of q is denoted as $\tilde{Q}_{\sin}$, as shown in Equation (12).

$$q = \bar{Q}_0 + \tilde{Q}_{\cos}\cos\xi + \tilde{Q}_{\sin}\sin\xi \tag{12}$$

where,

$$\begin{cases} \bar{Q}_0 = -v_d^+ i_d^+ + v_q^+ i_q^+ - v_d^- i_d^- + v_q^- i_q^- \\ \tilde{Q}_{\cos} = -v_d^+ i_q^- + v_q^+ i_d^- - v_d^- i_q^+ + v_q^- i_d^+ \\ \tilde{Q}_{\sin} = v_d^+ i_d^- + v_q^+ i_q^- - v_d^- i_d^+ - v_q^- i_q^+ \end{cases}$$

In HVDC transmission system, the presence of harmonic components in DC current order may result in voltage and power fluctuation, compromising the stability control of the AC-DC system. Hence, the fundamental components of three-phase voltage and current of the AC filter are substituted into

Equation (11). Then take the obtained DC component $\bar{Q}_0$ as the reactive power compensated by the AC filter Q_f.

C. Calculation of DC Current Order

In initial stage of fault recovery, the active power of converters is still at a low level. At this point, the reactive power consumed by the converter is far lower than that supplied by the AC filter, resulting in a large amount of excessive reactive power being injected into the AC system. When the AC system is less robust, transient overvoltage will occur; when the AC system is robust, voltage fluctuation may occur. The both conditions will cause surge to the equipment on both the AC and DC sides.

Therefore, it is expected that the exchange of reactive power Q_{ac_ref} between the converter station and the AC system can be maintained around the steady-state value. Combining Q_f, the expected reactive power consumption of the inverter Q_{I_ref} is substituted into Equation (2), we have the characteristics relationship showing DC current order I_{d_ref} varying as a function of U_{ac}. It allows the reactive power consumption of the converter to be controlled quantitatively during fault recovery, thereby improving recovery performance of the AC-DC system.

III. Limit Value of DC Current Order under Different AC Faults

In order to further investigate the impact of HVDC operating characteristics on DC current order, this section is developed to analyze the constraint relationship between DC current and AC bus voltage under different fault types by setting appropriate extinction angle γ and leading firing angle β and using the calculation equation for HVDC system under the quasi-steady state.

The equation of DC voltage of HVDC system under the quasi-steady state is given as:

$$\begin{cases} U_d = 2(\dfrac{3\sqrt{2}}{\pi}kU_{ac}\cos\gamma - \dfrac{3}{\pi}XI_d) \\ U_d = 2(\dfrac{3\sqrt{2}}{\pi}kU_{ac}\cos\beta + \dfrac{3}{\pi}XI_d) \end{cases} \tag{13}$$

Thus, DC current order can be calculated using:

$$I_d = \frac{2.7kU_{ac}(\cos\gamma - \cos\beta)}{\dfrac{12}{\pi}X} \tag{14}$$

During the transient process, both k and X in Equation (14) are constants. Therefore, DC current I_d is directly related to γ and β under different AC bus voltages U_{ac}. In particular, I_d is negatively related to γ and positively related to β. The relationship among γ, β and overlap angle μ can be expressed as $\beta=\gamma+\mu$. In case of AC faults on the inverter side, the inverter operates under the constant-extinction-angle control, with the extinction angle being generally taken as 15°. Under normal operating conditions of 12-pulse converters, μ is less than 30° [2]. In this section, by taking the CIGRE model as an example and substituting the extinction angle γ and leading firing angle β into Equation (14), one can solve the maximum value of DC current respectively under the three-phase fault condition and the single-phase fault condition.

A. Three-phase Fault Condition

Under the three-phase fault condition, γ is 15° and μ is generally in the range of 20°-25°. Here, μ is taken as 25° and then β is 40°. Substituting γ, β and the CIGRE model parameters into Equation (14), one can obtain the characteristic curve of DC current limit I_{dmax_three} varying as a function of U_{ac} under this condition, as shown in Fig.4. The function expression of the characteristic curve is given by:

$$I_{d\max\_three} = 1.0925U_{ac} \tag{15}$$

In Fig.4, when the voltage is higher, I_{dmax_three} is almost the same as the DC current of VDCOL. While the voltage is lower, I_{dmax_three} is much smaller than the DC current of VDCOL. Therefore, the DC current in the proposed control strategy can be reduced more quickly, and the reactive power consumed by the converter can also be reduced more quickly to balance the active power of converter station.

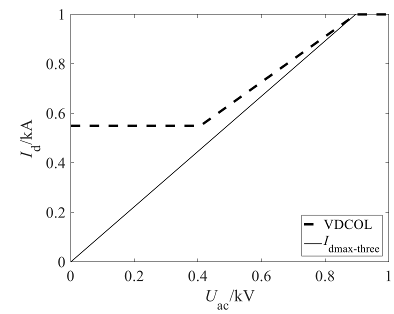

Fig.4 The comparison between the DC current of VDCOL and I_{dmax_three} under symmetrical conditions

B. Asymmetrical Fault Conditions

In case asymmetrical faults occur in the system, the zero-crossing of commutation voltage would shift. For example, in case of the grounding short-circuit fault of phase A, assume that the grounding impedance of the faulty phase is Z_f, the phase-to-neutral voltages and phase-to-phase voltages on the grid side of converter transformers following the fault can be calculated using Equations (16) and (17).

$$\begin{cases} \boldsymbol{v}_a' = \dfrac{3Z_f}{Z} \\ \boldsymbol{v}_b' = (-\dfrac{3Z_0+3Z_f}{2Z} - j\dfrac{\sqrt{3}}{2}) \\ \boldsymbol{v}_c' = (-\dfrac{3Z_0+3Z_f}{2Z} + j\dfrac{\sqrt{3}}{2}) \end{cases} \tag{16}$$

$$\begin{cases} \boldsymbol{v}_{ba}' = -\dfrac{9Z_f+3Z_0}{2Z} - j\dfrac{\sqrt{3}}{2} \\ \boldsymbol{v}_{cb}' = j\sqrt{3} \\ \boldsymbol{v}_{ac}' = \dfrac{9Z_f+3Z_0}{2Z} - j\dfrac{\sqrt{3}}{2} \end{cases} \tag{17}$$

where, $Z= Z_1+ Z_2+ Z_0+ 3Z_f$, Z_1, Z_2 and Z_0 are respectively the impedances at the short-circuit point in positive-sequence, negative-sequence and zero-sequence network.

As shown in Fig. 5, assuming that the phase of firing pulses remains unchanged, due to the decrease of the amplitude of v_{ba} and the zero-crossing being shifted forward by an angle φ, the firing angle is increased from α to $\alpha'=\alpha+\varphi$, the leading

This article has been accepted for publication in a future issue of this journal, but has not been fully edited. Content may change prior to final publication. Citation information: DOI 10.1109/TPWRD.2019.2892410, IEEE Transactions on Power Delivery

firing angle is reduced from β to $\beta'=\beta-\varphi$ and the extinction angle is reduced from γ to $\gamma'=\gamma-\varphi$ .Therefore, to obtain the maximum value of DC current under asymmetric fault condition, it is necessary to solve the variation characteristics of offset φ under different fault levels.

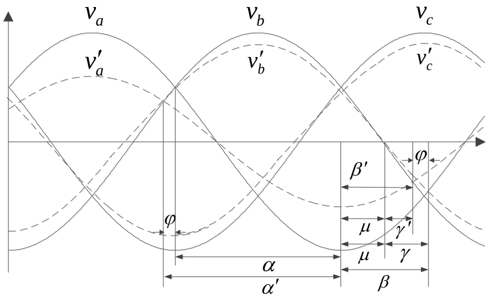

Fig.5 The offset of commutation voltage under single-phase faults

the RMS of phase-to-phase voltage of AC bus can be calculated using Equation (18).

$$U_{ac}=\frac{1}{3}(|\boldsymbol{v}_{ba}|^2+|\boldsymbol{v}_{cb}|^2+|\boldsymbol{v}_{ac}|^2) \tag{18}$$

As the wiring configurations of the converter transformers at upper and lower bridge of the 12-pulse converter are different and the amplitude and phase of AC voltage on the valve side of the converter transformers vary from one phase to another, it is necessary to investigate the offset of extinction angle of converter valve respectively for Yny0 and YnD1 connection mode.

1. Yny0 connection mode of converter transformer

In the case of Yny0 connection mode, the commutation voltage on the valve side of converter transformer can be expressed as:

$$\begin{cases} \boldsymbol{v}_{yba}=-\dfrac{3}{2}\dfrac{Z_0+3Z_f}{Z}-j\dfrac{\sqrt{3}}{2} \\ \boldsymbol{v}_{ycb}=j\sqrt{3} \\ \boldsymbol{v}_{yac}=\dfrac{3}{2}\dfrac{Z_0+3Z_f}{Z}-j\dfrac{\sqrt{3}}{2} \end{cases} \tag{19}$$

If $\dfrac{Z_0+3Z_f}{Z}$ is expressed in terms of $A+Bj$, then:

$$\begin{cases} \boldsymbol{v}_{yba}=-\dfrac{3}{2}A-(\dfrac{3B+\sqrt{3}}{2})j \\ \boldsymbol{v}_{ycb}=j\sqrt{3} \\ \boldsymbol{v}_{yac}=\dfrac{3}{2}A-(\dfrac{\sqrt{3}\text{-}3B}{2})j \end{cases} \tag{20}$$

Thus, the offset of the commutation voltage on the valve side of converter transformer can be expressed as:

$$\begin{cases} \Delta\varphi_{yba}=\arctan(\dfrac{3B+\sqrt{3}}{3A})-30° \\ \Delta\varphi_{ycb}=0 \\ \Delta\varphi_{yac}=30°-\arctan(\dfrac{\sqrt{3}-3B}{3A}) \end{cases} \tag{21}$$

The offset of the commutation voltage varies as a function of AC bus voltage U_{ac}, as shown in Fig. 6(a). Specifically, the phase of commutation voltage $\boldsymbol{v}_{yba}$ is advanced with respect to that of the normal case, while the phase of commutation voltage $\boldsymbol{v}_{yac}$ lags behind that of the normal case. Therefore, the maximum advanced offset $\Delta\varphi_Y$ of extinction angle of converter valve can be calculated using the following equation:

$$\Delta\varphi_Y=\arctan(\frac{3B+\sqrt{3}}{3A})-30° \tag{22}$$

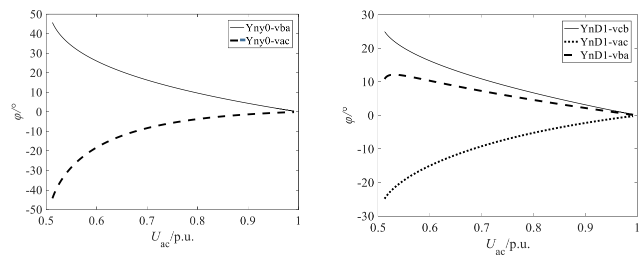

(a) Yny0 connection mode (b) YnD1 connection mode

Fig.6 The offset of commutation voltage under the different connection mode

2. YnD1 connection mode of converter transformer

The commutation voltage on the valve side of the converter transformer can be expressed as:

$$\begin{cases} \boldsymbol{v}_{\Delta ba}=-\sqrt{3}\dfrac{Z_0+3Z_f}{Z}=-\sqrt{3}A-\sqrt{3}Bj \\ \boldsymbol{v}_{\Delta cb}=\dfrac{\sqrt{3}}{2}\dfrac{Z_0+3Z_f}{Z}+j\dfrac{3}{2}=\dfrac{\sqrt{3}}{2}A+(\dfrac{\sqrt{3}B+3}{2})j \\ \boldsymbol{v}_{\Delta ac}=\dfrac{\sqrt{3}}{2}\dfrac{Z_0+3Z_f}{Z}-j\dfrac{3}{2}=\dfrac{\sqrt{3}}{2}A-(\dfrac{3-\sqrt{3}B}{2})j \end{cases} \tag{23}$$

Thus, the offset of the commutation voltage on the valve side of the converter transformer can be expressed as:

$$\begin{cases} \Delta\varphi_{\Delta ba}=\arctan(\dfrac{B}{A}) \\ \Delta\varphi_{\Delta cb}=\arctan(\dfrac{\sqrt{3}B+3}{\sqrt{3}A})-60° \\ \Delta\varphi_{\Delta ac}=60°-\arctan(\dfrac{3-\sqrt{3}B}{\sqrt{3}A}) \end{cases} \tag{24}$$

The offset of the commutation voltage changes as a function of AC bus voltage, as shown in Fig.6(b). Specifically, the phase of commutation voltages $\boldsymbol{v}_{\Delta ba}$ and $\boldsymbol{v}_{\Delta cb}$ are advanced with respect to the normal case while the phase of commutation voltage $\boldsymbol{v}_{\Delta ac}$ lags behind the normal case. Therefore, the maximum advanced offset $\Delta\varphi_\Delta$ of the extinction angle of converter valve can be calculated using the following equation:

$$\Delta\varphi_\Delta=\arctan(\frac{\sqrt{3}B+3}{\sqrt{3}A})-60° \tag{25}$$

In summary, the characteristic curve of the offset φ of the commutation voltage varied as a function of U_{ac} under two connection modes (Yny0 and YnD1) is shown in Fig.7(a).

This article has been accepted for publication in a future issue of this journal, but has not been fully edited. Content may change prior to final publication. Citation information: DOI 10.1109/TPWRD.2019.2892410, IEEE Transactions on Power Delivery

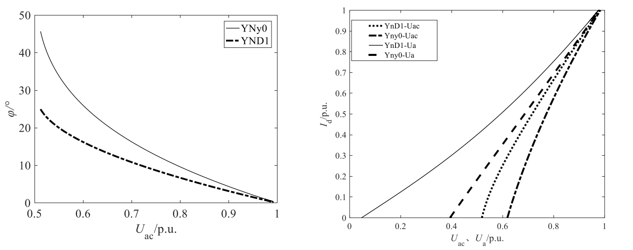

(a) the offset angle (b) the maximum value of DC current
Fig.7 Variation characteristics under the Yny0 and YnD1 connection mode

Under asymmetric fault conditions, in order to ensure normal operation of the system, the overlap angle is still taken as 25°, and the extinction angle shall be taken as 15°. Substituting Equations (22) and (25) and CIGRE model parameters into Equation (14), one can obtain the characteristics curve showing the maximum value of DC current varying as a function of AC bus voltage/fault phase voltage under this condition, as shown in Fig.7(b). For a 12-pulse converter, the maximum value of DC current shall be within the common zone of Yny0 and YnD1 connection modes. Then, the characteristics functions showing the change of DC current limit $I_{\mathrm{dmax\_single}}$ as the functions of the AC bus voltage U_{ac} and the fault phase voltage U_{a} under single-phase asymmetrical fault condition are given in Equation (26) and Equation (27) respectively.

$$I_{d\max\_\sin gle} = 9.82485U_{ac}^{3} - 26.8732U_{ac}^{2} + 26.68U_{ac} - 8.58 \quad (26)$$

$$I_{d\max\_\sin gle} = 1.735U_{a} - 0.698 \quad (27)$$

IV. Implementation of HVDC Recovery Strategy following AC Fault

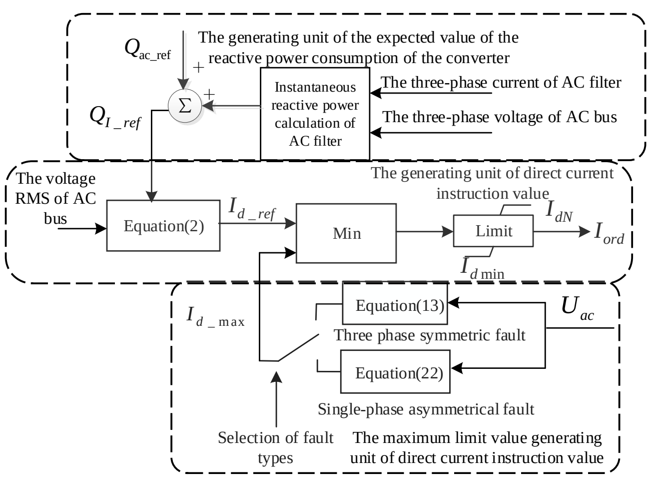

Fig.8 The method of AC fault recovery instead of the VDCOL of HVDC

From the above, DC current order of HVDC recovery strategy is shown in Fig.8. First, the HVDC control system takes samples of the AC bus voltage and current cyclically. When any fault is detected by the control system, the maximum limit of DC current order $I_{\mathrm{d\_max}}$ is solved in real time using Equation (15) or Equation (27). Meanwhile, the expected value $Q_{\mathrm{I\_ref}}$ of reactive power consumption of the inverter is calculated in real time as well to solve DC current order $I_{\mathrm{d\_ref}}$ under such condition. Finally, the smaller of $I_{\mathrm{d\_max}}$ and $I_{\mathrm{d\_ref}}$ is taken and the ultimate DC current order I_{ord} is determined by the amplitude limiter (in such limiter, I_{dN} is taken as 1.0p.u. and I_{dmin} is taken as 0.1p.u.). The HVDC control system executes this process cyclically until U_{ac} is restored and stable at the rated value.

V. Simulation And Validation

In this paper, the CIGRE benchmark model for HVDC controls is taken as an example. In the PSCAD/EMTDC simulation program, the proposed control strategy which is called "new way" in the plots, has been simulated and analyzed in the improvement of the system recovery performance, and compared with the VDCOL control.

A. Comparison in Respect of Commutation failure Immunity Performance

Commutation Failure Immunity Index (CFII) and Commutation Failure Probability Index (CFPI) can be used to measure the likelihood of commutation failure. It can be calculated using the following equation [20]:

$$CFII = \frac{P_{cf}}{P_{dcN}} \cdot 100\% = \frac{U_{acN}^{2}}{Z_{fault} P_{dcN}} \cdot 100\% \quad (28)$$

$$CFPI = \frac{\text{Frequency of commutation failure}}{\text{Total simulation times in each cycle}} \cdot 100\% \quad (29)$$

where, P_{cf} is critical power under fault, P_{dcN} is the rated power, U_{acN} is rated voltage of AC bus, and Z_{fault} is critical impedance in case of commutation failure. With a larger CFII or a smaller CFPI, the inverter is more robust to resist subsequent commutation failures.

The three-phase fault tends to cause more severe local damage than the single-phase to ground fault. Therefore, the three-phase short-circuit fault is simply taken as an example here to calculate the CFIIs and measure the fault recovery time for eleven short-circuit ratios (SCRs) and two control strategies (i.e., VDCOL and the control strategy proposed herein). Set 100 fault points uniformly within a period of 0.02s, each fault lasting for 0.1s. Solve the CFPIs of second commutation failure of the HVDC system respectively for the two control strategies. See Fig.9 for the results.

TABLE I
Comparison of Commutation Failure Immunity Performance

SCR	CFII/%		Fault Recovery Time/ms	
	VDCOL	New way	VDCOL	New way
2.5	31	117.5	127.1	41.7
3	42.43	176.3	185	48
3.5	52.9	230	200	52
4	58.8	230	235	100
4.5	75.5	251.9	230	80
5	132.25	352.6	200	80
6	151.14	440.83	240	100
7	170.64	440.83	250	80
8	195.93	440.83	260	100
9	230	529	255	90
10	293.89	529	250	86

It follows from Table 1 that with the increase of SCR, the AC-DC system becomes more robust in suppressing subsequent commutation failures of HVDC systems. For the same SCR, the CFIIs of the proposed control strategy is larger than that of the

This article has been accepted for publication in a future issue of this journal, but has not been fully edited. Content may change prior to final publication. Citation information: DOI 10.1109/TPWRD.2019.2892410, IEEE Transactions on Power Delivery

VDCOL control, indicating that the proposed control strategy can significantly improve the system ability to suppress subsequent commutation failures of HVDC systems. Moreover, the fault recovery time of the proposed control strategy is about 2 times less than that of the VDCOL control, verifying the superiority of the proposed control strategy in improving the system recovery performance over the VDCOL control. As shown in Fig.9, for the VDCOL control, the subsequent commutation failure is initiated when the AC bus voltage U_{ac} drops by 2.3% and is completed when it drops by 5%. While for the proposed control strategy, the subsequent commutation failure is initiated when the AC bus voltage U_{ac} drops by 15% and is completed when it drops by 35%. This indicates that the proposed control strategy can effectively improve fault ride-through performance of the AC-DC system to some degree.

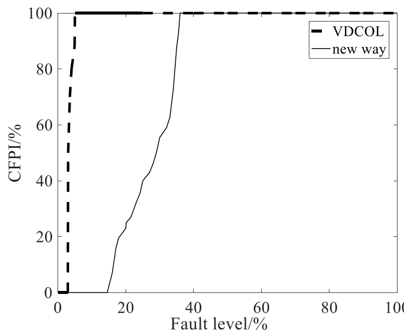

Fig.9 CFPIs for two control methods at SCR=2.5

B. Recovery Performance of the System in Case of Three-phase Faults

1. Tests for weak receiving AC system

The CIGRE benchmark model has a weak AC system at receiving end with the SCR of 2.5. Assume that a three-phase fault occurs at t=2s and is cleared 0.1s later, the critical impedance of commutation failure in the proposed control strategy is set as the three-phase grounding impedance, and the AC voltage drops to about 0.7p.u.. Through simulation analysis of the CIGRE model for the two control strategies, the active power (P_{dc}), the reactive power exchange (Q_{ac}), the AC bus voltage (U_{ac}), the DC voltage (U_d), the DC current order (I_{dc}), and the extinction angle (γ) are shown in Fig.10.

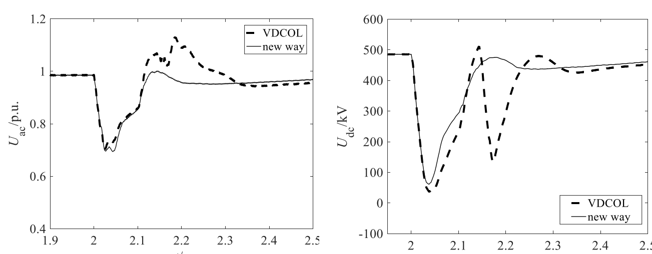

(a) AC bus voltage (b) DC voltage

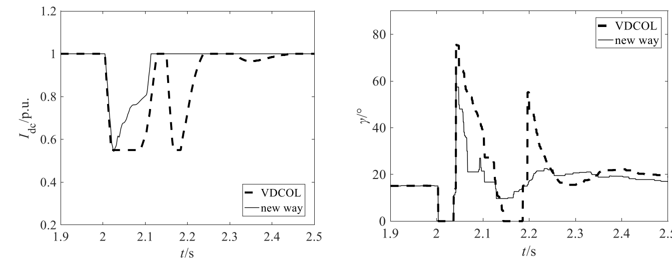

(c) DC current order (d) Extinction angle

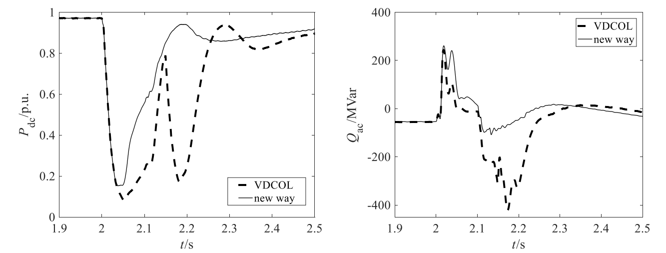

(e) Active power (f) Reactive power exchange

Fig.10 The recovery characteristics of AC-DC system under three-phase faults at SCR=2.5

It is concluded from the above simulation results that, as the AC system of CIGRE benchmark model is a weak system, the DC current recovery rate in the VDCOL control mode is slower than that in the proposed control strategy. A large quantity of excess reactive power supplied by the AC filter is injected into the AC system, causing the system overvoltage. The control on the inverter side switches from the constant-extinction-angle control to the constant-current control back and forth, and the DC current order oscillates. This is the root cause of the secondary commutation failure during fault recovery. In contrast, the proposed control strategy is targeted at the expected value of reactive power exchange of converter stations. It solves the expected value of converter reactive power consumption in real time to obtain the DC current order, which can well balance the reactive power of the converter station during fault recovery period.

2. Tests for strong receiving AC system

To further verify general applicability of the improved control strategy, increase the SCR of the receiving-end AC system of the CIGRE benchmark model to 10 and verify its effectiveness in controlling the strong receiving AC system. Likewise, assume that a three-phase fault occurs at t=2s and is cleared 0.1s later, the critical impedance of commutation failure at this SCR is set as the three-phase grounding impedance, and the AC bus voltage U_{ac} drops to about 0.8p.u. The response characteristics curves of the various electrical quantities are obtained through simulation as shown in Fig.11.

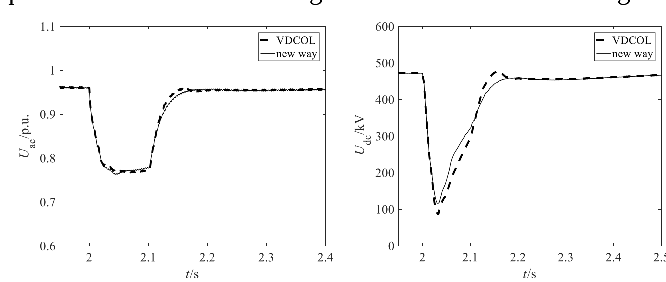

(a) AC bus voltage RMS (b) DC voltage

This article has been accepted for publication in a future issue of this journal, but has not been fully edited. Content may change prior to final publication. Citation information: DOI 10.1109/TPWRD.2019.2892410, IEEE Transactions on Power Delivery

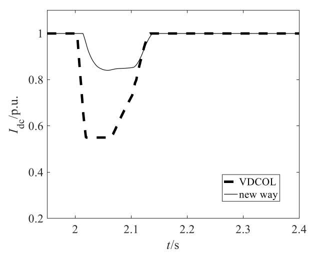

(c) DC current order

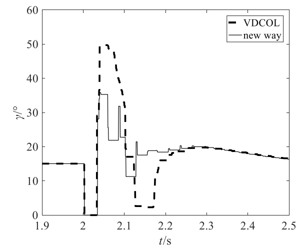

(d) Extinction angle

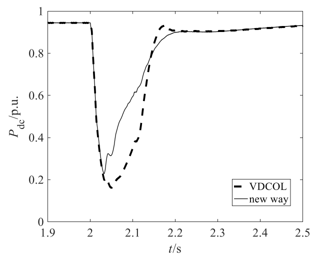

(e) Active power

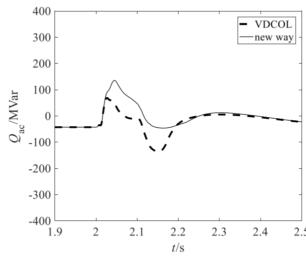

(f) Reactive power exchange

Fig.11 The recovery characteristics of AC-DC system under three-phase faults at SCR=10

In terms of AC bus voltage, the AC-DC system with a strong AC system at receiving end is more resistant to disturbances than that with a weak AC system at receiving end. For the two control strategies, the exchange of reactive power between the AC system and the converter station varies within a small range around the steady-state value, ensuring relatively stable voltage. The proposed control strategy is more capable of controlling the reactive power change steadily than the VDCOL control. By dynamically tracking the system recovery state to suppress the fluctuation of reactive power exchange, it can accelerate the recovery of DC current order so that is can match the system recovery state. This can not only meet the reactive power demand for the recovery of the AC voltage, but also improve the recovery characteristics of DC voltage and active power and enhance the system's capability of suppressing subsequent commutation failures.

C. Recovery Performance of the System under Single-phase Faults

1. Tests for weak receiving AC systems

Take a grounding short-circuit fault occurring on phase A for example in the CIGRE model which has a weak AC system at receiving end with the SCR of 2.5. Assume that the fault occurs at t=2s and is cleared 0.1s later. The voltage of faulty phase A drops to about 0.5p.u. after the fault. The response characteristics curves of the various electrical quantities are obtained through simulation as shown in Fig.12.

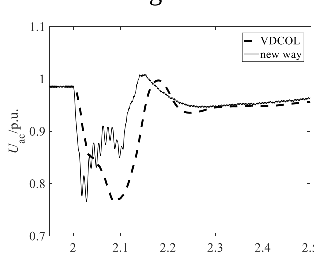

(a) AC bus voltage RMS

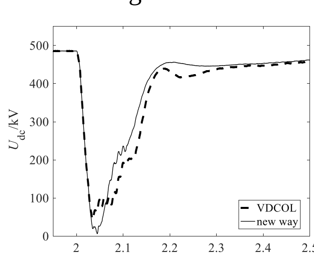

(b) DC voltage

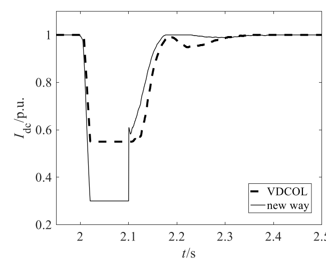

(c) DC current order

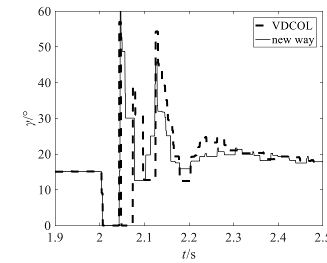

(d) Extinction angle

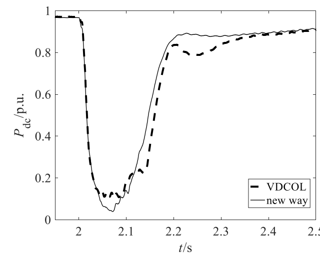

(e) Active power

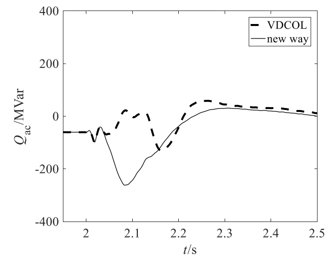

(f) Reactive power exchange

Fig.12 The recovery characteristics of AC-DC system under asymmetric faults at SCR=2.5

As shown in Fig. 12, the proposed control strategy has better fault recovery performance. The proposed control strategy can obtain the DC current order in real time through tracking the change of the faulty phase voltage. Compared with the VDCOL control, the proposed control strategy can feedback the fault characteristics of the AC system more quickly, allowing the control system to make response rapidly. Therefore, the proposed control strategy enables the AC voltage recovery more quickly than the VDCOL control.

2. Tests for strong receiving AC systems

Increase the SCR of the CIGRE model to 10 and the other fault conditions remain the same. The response characteristic curve of the various electrical quantities of the system are obtained through simulation as shown in Fig. 13.

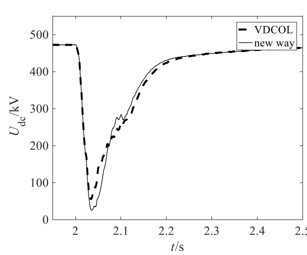

(a) AC bus voltage RMS

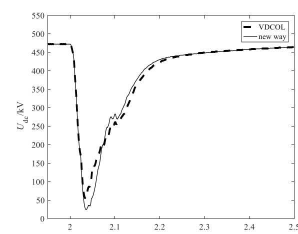

(b) DC voltage

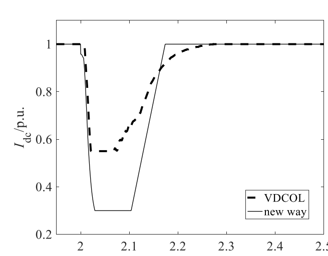

(c) DC current order

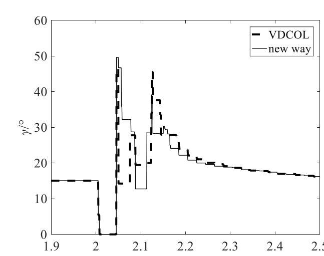

(d) Extinction angle

This article has been accepted for publication in a future issue of this journal, but has not been fully edited. Content may change prior to final publication. Citation information: DOI 10.1109/TPWRD.2019.2892410, IEEE Transactions on Power Delivery

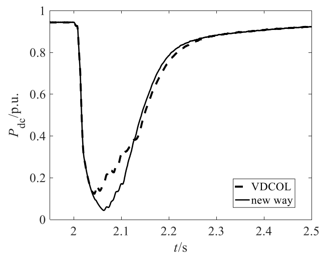

(e) Active power

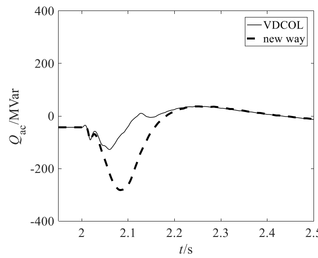

(f)Reactive power exchange

Fig.13 The recovery characteristics of AC-DC under asymmetric faults at SCR=10

It follows from Fig.13 that, for the strong AC system in the receiving end at SCR=10, the proposed control strategy can track the change of the voltage on faulty phase and enable the control system to respond more quickly. It is more sensitive to AC faults than the VDCOL control and is superior to the VDCOL control in terms of recovery performance. The DC current order obtained through the proposed control strategy is smaller than that obtained through the VDCOL control at the expense of some reduced active power transmission. In spite of this, the strong receiving AC system is strong enough to withstand the single-phase to ground fault and, as a result, the system recovery will not be affected adversely due to the reduced active power transmission.

In all, the proposed control strategy offers better control performance than the VDCOL control for the AC faults. This strategy can fully exploit reactive power regulation capability of the converter valves to control the exchange of reactive power of the converter station at the expected value accurately, thereby improving the recovery performance of DC voltage and AC bus voltage and reducing the probability of subsequent commutation failure during fault recovery of HVDC transmission system and, consequently, significantly enhancing the stability of the AC-DC system.

VI. Conclusion

In this paper, the operating characteristics of HVDC system after AC faults are analyzed and a fault recovery strategy in lieu of traditional VDCOL is proposed. This recovery strategy can not only ensure the reactive power balance of converter stations, but also be helpful in the recovery of AC bus voltage. The main works completed in this paper are as follows:

1)The characteristic relationship among the AC bus voltage, the reactive power of converter station and the DC current order is analyzed, and the drawbacks of VDCOL control are investigated in order to develop a method for solving DC current order based on the AC bus voltage on condition of controlling reactive power exchange of converter stations at the expected value.

2) Calculate the expected reactive power consumption of converters on real-time basis in response to the AC bus voltages and currents such that the recovery rate of DC current order can match with the recovery state of the AC system.

3) Research the change characteristics of the firing angle respectively under the three-phase fault and the single-phase fault and calculate the maximum value of DC current as a function of the AC bus voltage.

4) Take the CIGRE benchmark model for HVDC controls as an example and develop the simulation tests by assuming that the SCR is 2.5 and 10 respectively. The results show that the recovery strategy proposed in this paper can significantly reduce the probability of subsequent commutation failures of HVDC systems and improve the recovery performance of AC-DC systems.

References

[1] L. Herman, A. Bozicek, B. Blazic, L. Papic, "HVDC technology and power quality issues in Slovenian transmission system – technical study," in *Proc. 24th int. Conf. & Exhi. On Electricity Distribution*, vol.2017, no.1, 2017, pp.700-704.

[2] Zhao Wanjun. "High voltage direct current transmission engineering," Beijing: China Electric Power Press, 2010.

[3] K.R. Padiyar, *HVDC Power Transmission Systems: Technology and System Interactions*, Wiley, 1990.

[4] Bui M X, Mai H N, Saha T K. "Dynamic simulation of HVDC interconnection in large power system," in *Proc. IEEE Power &Energy Soc. General Meeting*, 2011, pp.1-7.

[5] C.V. Thio, J.B. Davies, K.L. Kent, "Commutation failures in HVDC transmission systems", *IEEE Trans. on Power Del.*, vol. 11, no. 2, pp. 946-957, Apr. 1996.

[6] D.L.H. Aik, G. Andersson, "Voltage stability analysis of multi-infeed HVDC systems," *IEEE Trans. on Power Del.*, vol.12, no.3, pp.1309-1318, Jul. 1997 .

[7] FU Ying, LUO Longfu, TONG Ze, *et al*., "Study on Voltage Dependent Current Order Limiter of HVDC Transmission System' s Controller," *High Voltage Engineering*, vol.34, no.6, pp.1110-1114, Jun. 2008.

[8] M.H. Nguyen, T.K. Saha, M. Eghbal, "Master self-tuning VDCOL function for hybrid multi-terminal HVDC connecting renewable resources to a large power system," *Iet Generation Transmission & Distribution*, vol.11, no.13, pp.3341-3349, Sept. 2017.

[9] C.Y. Guo, Y.C. Liu, C.Y. Zhao, X.G. Wei, W.H. Xu, "Power Component Fault Detection Method and Improved Current Order Limiter Control for Commutation Failure Mitigation in HVDC," *IEEE Trans. on Power Del.*, vol.30, no.3, pp.1585-1593, Mar. 2015.

[10] Zheng Chao, Zhou Jingmin, Li Huiling, *et al*., "Impact of Commutation Failure Prediction Control on Voltage Stability and Its Optimization Measures," *Automation of Electric Power Systems*, vol.40, no.12, pp.179-183, 2016.

[11] C. Zheng, S.Y. Ma, C.H. Sheng, X.J. Guo, *et al*., "Transient Voltage Stability Control Based on the HVDC Inverter Station Acting as Dynamic Reactive Source," *Proceedings of the CSEE*, vol.34, no.34, pp.6141-6149, 2014.

[12] H. RAO, S.K. XU, Y. ZHAO, C. HONG, W. WEI, X.L. LI, J.S. ZHANG, Q. SONG, "Research and application of multiple STATCOMs to improve the stability of AC/DC power systems in China Southern Grid," *IET Gener., Transm. & Distrib.*, vol. 10, no. 13, pp. 3111-3118, Oct. 2016.

[13] Y. Xue, X.P. Zhang, "Reactive Power and AC Voltage Control of LCC HVDC System With Controllable Capacitors," *IEEE Trans. on Power Syst.*, vol.32, no.1, pp.753-764, May 2017.

[14] C.H. Li, Y. Huang, M. Li, R.B. Cao, "An Optimal Control Strategy to Mitigate Commutation Failure of HVDC," *Southern Power System Technology*, vol.11, no.6, pp.1-7, Jun. 2017.

[15] C.K. Kim, "Dynamic coordination strategies between HVDC and STATCOM," in *Proc. Transm. & Distrib. Conf. & Exposi.: Asia and Pacific*, 2009, pp. 1-9.

[16] J.J. Wang, Z.Y. Liang, Z.L. Li, Y.J. Li, C. Fu, L.B. Huang, "Reactive Power Control Strategy for Low Power Operation of HVDC Transmission System," *Automation of Electric Power System*, vol. 41, no. 6, pp.154-158, Mar. 2017.

[17] B.R. Zhou, Z.B. Du , D.H. Luo , L.Y. Liu , F.J. Zhan. " VDCOL Parameters Design of Multi-infeed HVDC Based on A Simplified Model of DC P-Q Coupling Recovery," in *Proc.* IEEE PES Asia-Pacific Power and Energy Engineering Conference (APPEEC), 2014, pp. 1-5.

This article has been accepted for publication in a future issue of this journal, but has not been fully edited. Content may change prior to final publication. Citation information: DOI 10.1109/TPWRD.2019.2892410, IEEE Transactions on Power Delivery

[18] M.H Huang, J.J. Wang, Y.J. Li, Z.L. Li, C. Fu,, "Constant Reactive Power Control During AC Fault Recovery for HVDC," Automation of Electric Power Systems, vol.42, no.3, pp.143-148, Feb. 2018.

[19] H. Akagi, Y. Kanazawa, A. Nabae, "Instantaneous reactive power compensators comprising switching devices without energy storage components," IEEE Trans. on Ind. Appli., vol.20, no.3, pp.625-630, May 1984.

[20] E. Rahimi, A. Gole, B. Davies, L. Fernando, K. Kent, "Commutation Failure Analysis in Multi-Infeed HVDC Systems," IEEE Trans. on Power Del., vol.26, no.1, pp.378-384, Dec. 2011.

Juanjuan Wang received the M.S. degree from Huazhong University of Science and Technology, Wuhan, China, in 2003 and the Ph.D. degree from South China University of Technology, Guangzhou, China, in 2009.She currently is a Professor at South China University of Technology. Her research interests include FACTS, power system analysis and voltage stability, and operation of power systems.

Menghua Huang was born in Fujian Province, China, on July 8, 1994. She received the B.S. degree from Central South University, Changsha, China, in 2012. Currently, she is a graduate student in the School of Electric Power, South China University of Technology, Guangzhou, China.

Chuang Fu (M'15) received the B.S. degree in hydro-electrical engineering from Sichuan Institute of Technology, Chengdu, China, in 1996 and the M.S. and Ph.D. degrees in electrical engineering from Huazhong University of Science and Technology, Wuhan, China, in 1999 and 2003, respectively. He has been with the Electric Power Research Institute, China Southern Power Grid since 2005.

Huan Li received the B.S. degree in electrical and electronic engineering from Huazhong University of Science and Technology, Wuhan, China, in 2008 and the Ph.D. degree in power system and its automation from Huazhong University of Science and Technology, Wuhan, China, in 2014. He has been with the Electric Power Research Institute, China Southern Power Grid since 2014.

Shukai Xu (SM'18) received the B.S. and Ph.D. degrees in electrical engineering from Tsinghua University, Beijing, China, in 2002 and 2007, respectively. He is currently a Principal Engineer with the Electric Power Research Institute of China Southern Power Grid, Guangzhou, China. He is a Fellow of IET and his main research interests are in flexible ac transmission systems and HVDC.

Xiaohua Li received the B.E. and Ph.D. degrees in electrical engineering from Huazhong University of Science and Technology, China, in 1997 and 2003 respectively. Now, she is a Professor in school of electric power, South China University of Technology, Guangzhou, China. Her research interests are in power system fault analysis and relay protection, HVDC power transmission operation technology.